Proceedings of the VIII International Conference ION 2010, Kazimierz Dolny, Poland, June 14–17, 2010

Magnetoresistance in n-Si/SiO$_2$/Ni Nanostructures Manufactured by Swift Heavy Ion-Induced Modification Technology

J. Fedotova[a,*], D. Ivanou[b], Y. Ivanova[b], A. Fedotov[b], A. Mazanik[b], I. Svito[b], E. Streltsov[b], A. Saad[c], S. Tyutyunnikov[d], T.N. Kołtunowicz[e], S. Demyanov[f] and V. Fedotova[f]

[a]National Center of Particles and High Energy Physics of BSU, 153 Bogdanovich, 220040 Minsk, Belarus

[b]Belarussian State University, 4 Independence, 220030 Minsk, Belarus

[c]Al-Balqa Applied University, P.O. Box 2041, Amman 11953, Salt, Jordan

[d]Joint Institute for Nuclear Research, 6 Joliot-Curie, 141980 Dubna, Russia

[e]Lublin University of Technology, Nadbystrzycka 38a, 20-618 Lublin, Poland

[f]Scientific-Practical Material Research Centre NAS of Belarus, 19 P. Brovka, 220072, Minsk, Belarus

A study of magnetotransport in the n-Si/SiO$_2$/Ni nanostructures with granular Ni nanorods in SiO$_2$ pores was performed over the temperature range 2–300 K and at the magnetic fields induction up to 8 T. The n-Si/SiO$_2$/Ni Schottky nanostructures display the enhanced magnetoresistive effect at 25 K due to the impurity avalanche mechanism.

PACS: 68.55.Ln, 81.05.Rm, 73.22.−f, 73.50.Jt

1. Introduction

At present, a special interest is aroused in the development of nanostructures exploiting the enhanced magnetoresistive effects [1]. One of the approaches to the fabrication of such structures is based on the porous template-assisted synthesis, in the process of which nanopores in SiO$_2$, Al$_2$O$_3$, and the like are filled with different nanostructured substances [2]. Very often such fabrication is based on the nuclear ion track etch method (NITEM), where selective etching of the latent ion tracks leading to the creation of pores with a large length-to-diameter ratio enables one to form porous templates. Moreover, deposition of nanorods onto semiconductor substrates and application of an additional electrode enables the introduction of such nanostructures to MOSFET-like electronic elements called the TEMPOS structures [3, 4].

Of particular interest is the use of the NITEM technology for the fabrication of nanodevices by the electrodeposition procedure leading to the formation of high-quality deposits of the desired material within the pores [5].

In this work we compare the magnetotransport properties in the Ni nanogranular films deposited on the n-Si substrate and in the bundles of Ni nanorods embedded into the n-Si/SiO$_2$ porous template.

2. Experimental

In the present work we have used electrodeposition of Ni nanoparticles into the mesopores in a SiO$_2$ layer as a template created on the n-Si(100) substrate with 4.5 Ω cm resistivity to produce the magnetosensitive nanostructures n-Si/SiO$_2$/Ni. The regimes of mesoporous SiO$_2$ layer production by the NITEM technology were described in [6]. These nanopores having the diameters 100–250 nm and heights about 400–500 nm were filled with Ni to form a system of nanorods-in-pores (NRIPs) randomly distributed within the SiO$_2$ layer.

To separate the influence of Ni nanorods and Si/SiO$_2$ interface from the magnetoresistive effect of the n-Si/SiO$_2$/Ni nanostructures, we have also studied the magnetotransport properties in Ni films electrochemically deposited on the n-Si substrates at the same regimes as for the n-Si/SiO$_2$/Ni nanostructures. A thickness of the films with the granules measuring approximately 10–70 nm was close to the height of Ni-NRIPs in n-Si/SiO$_2$/Ni nanostructures (≈ 500 nm). The procedures of Ni electrodeposition into the pores together with their SEM images were presented in our previous paper [6].

The I–V characteristics and equilibrium DC resistances $R(V \to 0) = R_0$ of Ni films and n-Si/SiO$_2$/Ni nanostructures were measured by the two-probe method at temperatures 2–310 K and in magnetic fields B up to 8 T. See insets in Figs. 1a and 2 for the arrangement of the probes and orientations of the vectors of induction B and current I with respect to the substrate plane. As can be seen, the vector B both for Ni films and n-Si/SiO$_2$/Ni structures was directed either normally to (configuration 1) or along (configuration 2) the plane of Si substrate but B was always normal to I. A magnetoresistance (MR) of the samples studied was calculated by the well-known relation

* corresponding author; e-mail: fedotov@bsu.by

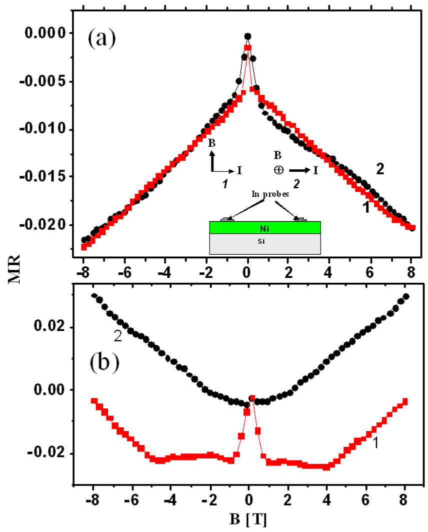

Fig. 1. MR_1 (1) and MR_2 (2) of Ni film vs. magnetic field induction B for temperatures $T = 300$ K (a) and 1.8 K (b). Two differing mutual orientations of B, I and substrate (film) plane, marked by numbers 1 and 2, and the corresponding measurements of MR_1 (1) and MR_2 (2) are shown in the inset in Fig. 1a.

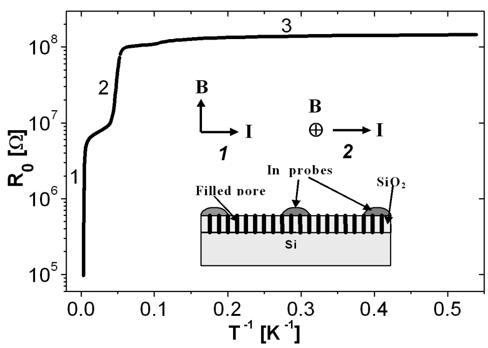

Fig. 2. Temperature dependence of resistance for a typical n-Si/SiO$_2$/Ni nanostructure: 1 — band conduction, 2 — impurity conduction, 3 — hopping conduction. The inset shows a schematic diagram of the sample containing Si substrate, SiO$_2$ layer with the Ni-filled pores, and two In electric probes. Two different mutual orientations of B, I and substrate plane in the inset are marked by numbers *1* and *2*.

$\mathrm{MR} = \Delta R/R(0) = [R(B) - R(0)]/R(0)$, where $R(B)$ and $R(0)$ were resistances with and without a magnetic field, respectively.

3. Results and discussion

3.1. Ni films

The Ni samples displayed a typical metallic behaviour with a power-like increase of the resistance with the temperature $R(T)$ in the temperature range 2–310 K due to phonon scattering of the electrons. As follows from Fig. 1, a behaviour of the MR(B,T) curves for Ni films can be explained by the competition of negative and positive contributions to MR. At $T > 250$ K the negative contribution dominated, exhibiting a linear increase of MR(B) modulus. The observed behaviour of negative-contribution MR with temperature and magnetic field could be attributed to the anisotropic magnetoresistance effect (AMR) due to scattering of the carriers on the magnetic spins of Ni atoms which are ordered at the temperature decrease [7]. At $T < 200$ K the films exhibited the usual positive Lorentz-like contribution to MR that increased with B and temperature lowering. Besides, the MR(B) curves for this temperature range begin to depend on the B–I-substrate plane orientation (see Fig. 1b).

3.2. n-Si/SiO$_2$/Ni nanostructures

The typical Arrhenius plot for the temperature dependences of the equilibrium resistance $R_0 = R_{V\to 0}(T)$ for the n-Si/SiO$_2$/Ni nanostructures is shown in Fig. 2. As suggested by the observed behaviour of the curves $\lg(R_0)$ vs. $(1/T)$, in the studied nanostructures at $T > 250$ K (region 1 in Fig. 2) the activation carrier transport by the Si substrate was dominant, giving the activation energy close to $E_g/2$ for the Si substrate. $R_0(T)$ for the region 2 (20–150 K) displayed the activation energy close to the phosphorus ionization energy in Si and could be attributed to the impurity conductance by the n-Si substrate. At $T < 15$ K (region 3), when the carrier transport by the Si substrate was freezed out, $R_0(T)$ was attributed in [8] to hopping of the carriers by the localized interfacial states within the space charge region (SCR), enriched by electrons, that has originated due to the band bending at the n-Si/SiO$_2$ interface.

Our measurements demonstrated that the I–V characteristics of n-Si/SiO$_2$/Ni nanostructures exhibited a change in their behavior from a linear (ohmic) in the temperature region 1 to the nonlinear and practically symmetric one at lower temperatures (see curve 1 in Fig. 3a). This low-temperature nonlinearity may be easily explained if we take into account that two bundles of nanorods, formed under the electric probes and joined by the Si substrate, electrically resemble two Si/Ni Schottky diodes switched on opposite to each other.

As can be seen in Fig. 3a, application of a magnetic field in both configurations 1 and 2 (normally and along the Si/SiO$_2$ interface of the n-Si/SiO$_2$/Ni nanostructure) of the B–I substrate plane caused an increase of resistance. Note that this effect was less pronounced for configuration 2 in the inset in Fig. 2, when B was normal to both I and Ni nanorods. Using the dependences of I–V on the magnetic field B, the magnetoresistance was estimated as $\mathrm{MR} = \Delta R/R_0 = [R(B) - R(0)]/R(0)$ with $R = V/I$ at $I = \mathrm{const}$. For example, for configuration 1 of the B–I substrate, when B was normal to both I and substrate and hence parallel to the Ni nanorods, the $MR_1(T)$ dependence for different measuring currents is given in Fig. 3b. As seen, at $T > 120$ K, where a zone

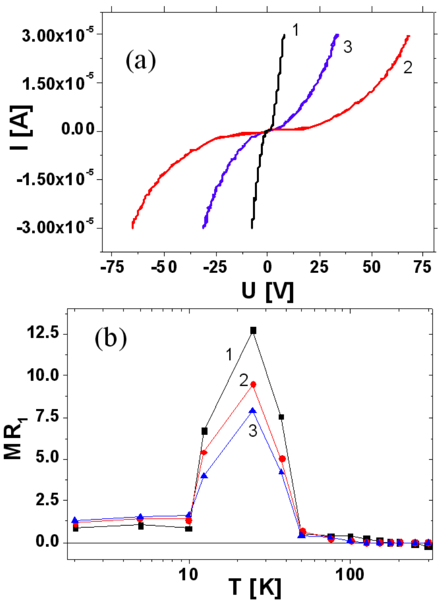

Fig. 3. *I–V* characteristics at 25 K for the magnetic field inductions $B = 0$ (1) and $B = 8$ T directed either normally (2) or along (3) the Si/SiO$_2$ interface (a); the temperature dependences of magnetoresistance $[R(8\text{ T}) - R(0)]/R(0)$ estimated for 3 different values of the measuring current I (b): 1 — 1 μA, 2 — 15 μA, 3 — 30 μA.

conductance by the Si substrate was predominant (region 1 for R_0 (T) in Fig. 2), the values of MR$_1$ were negative as for the samples of Ni films. This probably means that MR in this temperature region was due to the AMR effect in Ni nanorods (as described above for Ni films) because a positive Lorentz-like contribution into MR of the Si substrate was very low at these temperatures. At temperatures lower than 100 K the values of MR$_1$ for n-Si/SiO$_2$/Ni nanostructures were always positive. Moreover, we have observed a very strong enhancement of the positive MR effect at the temperatures 15–40 K (see also [8]).

As seen from Fig. 3b, the MR$_1(T)$ curves were strongly dependent on the value of measuring current, reaching their maximal values 80–1250% at approximately 25 K (see also [8]). Let us note that this enhanced MR just falls within the temperature region 2 in Fig. 2, where the impurity conductance was predominant and could be attributed to the Schottky-barrier impurity avalanche, as it was observed for the Au/GaAs structures [9].

4. Conclusion

In the n-Si/SiO$_2$/Ni nanostructures at the temperatures ranging from 15 to 40 K, where the impurity conductance by the phosphorus-doped Si substrate was predominant, an enhanced positive contribution to the MR effect was observed, that may be attributed to a mechanism of impurity avalanche in the Schottky n-Si/Ni structure.

Acknowledgments

The work was partially supported by the VISBY Program of the Swedish Institute, the Joint Institute for Nuclear Research (Dubna, Russia), the Belarussian State Scientific Program "NANOTECH", and the Belarussian Foundation for Fundamental Research.

References

[1] Y. Imry, in: *Nanostructures and Mesoscopic Systems*, Eds. W.P. Kirk, M.A. Reed, Academic, New York 1992, p. 11.

[2] H. Shang, G. Cao, in: *Springer Handbook of Nanotechnology*, Ed. B. Brushan, Springer, Berlin 2007, p. 161.

[3] D. Fink, A.V. Petrov, K. Hoppe, W.R. Fahrner, R.M. Papaleo, A.S. Berdinsky, A. Chandra, A. Chemseddine, A. Zrineh, A. Biswas, F. Faupel, L.T. Chadderton, *Nucl. Instrum. Methods Phys. Res. B* **218**, 355 (2004).

[4] D. Fink, D. Sinha, J. Opitz-Coutureau, A.V. Petrov, S.E. Demyanov, W.R. Fahrner, K. Hoppe, A.K. Fedotov, L.T. Chadderton, A.S. Berdinsky, in: *Physics, Chemistry and Application of Nanostructures (Reviews and Short Notes to Nanomeeting — 2005, Minsk, Belarus 2005)*, Eds. V.E. Borisenko, S.V. Gaponenko, V.S. Gurin, World Scientific, Singapore 2005, p. 474.

[5] E.A. Streltsov, N.P. Osipovich, L.S. Ivashkevich, A.S. Lyakhov, *Electrochim. Acta* **44**, 2645 (1999).

[6] Yu.A. Ivanova, D.K. Ivanou, A.K. Fedotov, E.A. Streltsov, S.E. Demyanov, A.V. Petrov, E.Yu. Kaniukov, D. Fink, *J. Mater. Sci.* **42**, 9163 (2007).

[7] B.M. Askerov, *Electron Transport Phenomena in Semiconductors*, World Sci., Singapore 1994.

[8] A. Fedotov, D. Ivanou, Y. Ivanova, A. Mazanik, I. Svito, A. Saad, S. Tyutyunnikov, S. Demyanov, V. Fedotova, in: *Abstracts of Forth Seeheim Conference on Magnetism SCM 2010, Karlsruhe Institute of Technology*, 2010, p. 52.

[9] A. Loukashevich, V.A. Grishanov, *Devices Control Syst.* **4**, 40 (1992).